Phase Contours of Scattering Amplitudes. III. High-Energy Behavior at Fixed Angles*

RICHARD J. EDEN† AND CHUNG-I TAN
Lawrence Radiation Laboratory, University of California, Berkeley, California 94720
(Received 18 March 1968)

The method of phase contours is applied to some problems concerned with scattering at fixed angles. The crossing-symmetric generalized Regge model developed in a previous paper is used to illustrate possible characteristics of the behavior of scattering amplitudes. These characteristics are discussed both in the complex energy plane at fixed angle and in the complex $\cos\theta$ plane at fixed high energy. The former leads to a procedure for studying fixed-angle behavior by means of entire functions on whose orders some limits can be established. The latter leads to a generalization of the lower bounds on high-energy behavior obtained earlier by Cerulus and Martin, and by Chiu and Tan.

1. INTRODUCTION

OUR main purpose in this paper is to show how the method of phase contours can be used in the problem of fixed-angle scattering at high energy. In particular, we will show that it gives a new way of formulating the problem, which is relevant to an heuristic approach and may also be used for a rigorous discussion of assumptions and consequent bounds on the high-energy behavior.

We will make extensive use of results and techniques on phase contours that were developed in the two previous papers[1,2] (hereafter denoted by I and II). In particular, we will use the crossing-symmetric model developed in II as a basis for formulating our discussion of fixed-angle behavior. This model is based on dominance by Regge-pole terms that correspond to rising trajectories. We use our knowledge of phase contours and zeros in this model to indicate the kind of behavior that should be taken into account in a more general discussion of high-energy behavior at fixed angles. Two essentially different approaches are considered. The first is directed towards the use of entire functions to describe the main features of scattering at a fixed angle. The second approach makes use of modulus contours in the complex $\cos\theta$ plane at high energy and can be used to obtain a fixed-angle lower bound.

In Sec. 2, we express the scattering amplitude for our model at fixed momentum transfer in terms of a Herglotz function and a ratio of polynomials in the energy. These polynomials are related to zeros of the scattering amplitude on the physical sheet and to phase contours on the boundary of the physical sheet. In Sec. 3 this result is generalized to fixed-angle behavior, where the polynomials become replaced by entire functions. The orders of the entire functions can be related to the distribution of zeros and the distribution of phase contours. If the entire function giving the zeros is dominant at high energies, then its order must be greater than or equal to one half.

In Sec. 4 we study the behavior of modulus contours for the amplitude in the complex $\cos\theta_t$ plane, where θ_t is the scattering angle. By considering the limiting form of these contours at high energy in our model, we see that polynomial boundedness in energy will in general be limited to a finite part of the $\cos\theta_t$ plane. This indicates the need for a generalization of the method for obtaining lower bounds that was first developed by Cerulus and Martin. The generalization is described in Sec. 5.

2. PHASE CONTOURS FOR A CROSSING-SYMMETRIC MODEL

In paper II, we developed solutions for phase contours from a Regge model that satisfies certain consistency tests under crossing symmetry. The starting point for the model is the assumption that the (equal-mass-boson) scattering amplitude has the asymptotic form, as $s\to+\infty$,

$$F(s,t)\sim\frac{b(t)s^{\alpha(t)}\exp[i\pi\{1-\frac{1}{2}\alpha(t)\}]}{\sin[\frac{1}{2}\pi\alpha(t)]\Gamma[\alpha(t)]}. \tag{2.1}$$

In our model we assume that the Regge trajectory $\alpha(t)$ rises continuously as t increases, and falls as t decreases. We also assume single pole dominance in the asymptotic limit $s\to+\infty$ for fixed t, except at zeros of the residue, that come from poles of the γ function at

$$\alpha(t)=-(2n+1). \tag{2.2}$$

There are two essentially different types of behavior for crossing-symmetric phase contours on the physical sheet that depend on the relative behavior of the leading Regge pole (2.1) and the next Regge pole. These two types of behavior were denoted A and B in Sec. 5 of II. We will find that with type A there is an infinite sequence of zeros on the physical sheet at fixed angles, whereas with type B this sequence of zeros of the scattering amplitude lies on unphysical sheets. There may be mixtures of the two types but, in order to avoid

* Work supported by the U. S. Atomic Energy Commission.
† Present address: Cavendish Laboratory, Cambridge, England.
[1] C. B. Chiu, R. J. Eden, and C.-I Tan, Phys. Rev. **170**, 1490 (1968). This paper is denoted I in the text.
[2] R. J. Eden and C.-I Tan, Phys. Rev. **170**, 1516 (1968). This paper is denoted II in the text.

an unduly long discussion, we will limit ourselves to the unmixed types.

In this section we will describe the characteristics of the phase contours in our model at fixed momentum transfer, and will use them to relate the scattering amplitude to a Herglotz function. In Sec. 3 we make the analogous steps at fixed angle.

Phase Contours

The phase $\phi(s,t)$ of the scattering amplitude $F(s,t)$ is defined by

$$\phi(s,t)=\mathrm{Im}\{\ln[F(s,t)]\}, \tag{2.3}$$

together with a specification of the route to the point (s,t) from the asymptotic forward direction, where we define our initial phase,

$$\phi(s\to\infty, t=0)=\tfrac{1}{2}\pi. \tag{2.4}$$

An account of theoretical and experimental properties of phase contours was given in I. Using these properties we developed the crossing-symmetric solutions of types A and B in II (Secs. 5 and 7), based on Eq. (2.1) above. We will discuss case B first since it is somewhat simpler than A.

Case B

The phase contours in the real s, real t, plane for type B are shown in Fig. 1 [see Fig. 17 of II]. The important features are: (1) The phase oscillates between π and 2π in the region

$$u>4m^2, \quad t>4m^2; \tag{2.5}$$

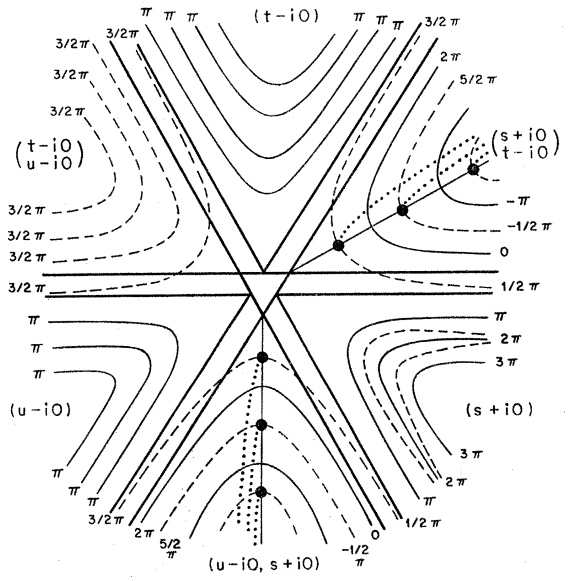

FIG. 1. Phase contours in the real (s,t,u) plane, for a crossing-symmetric amplitude based on the generalized Regge model. The small black circles indicate real zeros and the dotted lines indicate complex zeros. The phase contours and zeros correspond to case B discussed in the text.

(2) the phase in the region,

$$u<0, \quad t<0, \tag{2.6}$$

increases as s increases. For fixed negative t and large s, its approximate value is

$$\phi(s,t)\approx\pi[1-\alpha(t)]. \tag{2.7}$$

The correction term has magnitude less than $\frac{1}{2}\pi$. The difference between this phase (2.7) and the phase in the exponent in Eq. (2.1) is due to the zeros of the residue and the effects of the next highest Regge trajectory. The relation between the phase contours shown in Fig. 1 and the high-energy behavior for fixed negative t has been discussed in II (Sec. 5). We will be concerned with the corresponding relation at fixed angle. However it is useful to note first some features that apply to the simpler case of fixed t.

In Fig. 1, the small black circles denote real zeros of the amplitude, and the attached dotted curves denote complex zeros. In case B, which we are now considering, these zeros remain on the physical sheet, in the complex s plane, as t decreases through real values. In addition, zeros come in from infinity each time t decreases through a zero of the residue given by a solution of Eq. (2.2). These zeros also remain on the physical sheet as t decreases.

We consider the behavior of $F(s,t)$, for some fixed real negative value of t, as a function of s. There will be a finite number of zeros in $\mathrm{Im}s>0$, at

$$a_1(t), a_1(t), a_3(t), \cdots, a_l(t). \tag{2.8}$$

These can be factored out from F, giving

$$F(s,t)=\prod_1^l(s-a_r)G(s,t). \tag{2.9}$$

The function $G(s,t)$ will have phase contours that determine the oscillations through zero of $\mathrm{Im}G(s,t)$. Let the zeros of $\mathrm{Im}G(s,t)$ for real s (along $s+i0$) occur at

$$b_1(t), b_2(t), \cdots, b_m(t), \tag{2.10}$$

and at

$$c_1(t), c_2(t), \cdots, c_n(t), \tag{2.11}$$

where $b_i(t)$ denote points at which the phase of G increases through a value $N_0\pi$ as s increases, and $c_j(t)$ denotes points at which it decreases. Then, as described in I (Secs. 2 and 4), we can write $G(s,t)$ in the form

$$G(s,t)=\Big[\prod_1^m(s-b_i)/\prod_1^n(s-c_j)\Big]H(s,t), \tag{2.12}$$

where $\pm H$ is a Herglotz function of s, and satisfies

$$C/|s|<|H(s,t)|<C'|s|, \tag{2.13}$$

for some C and C' as $s\to\infty$, in $\mathrm{Im}s>0$.

The scattering amplitude F can therefore be written

in the form

$$F(s,t)=[P_a(s)P_b(s)/P_c(s)]H(s,t), \qquad (2.14)$$

where P_a, P_b, P_c denote polynomials whose order and coefficients depend on the chosen real value of t. In our model, when $\alpha(t)$ is near a negative even integer, $-2N$ say, the order of these polynomials will be $N+N'$, 0, and $3N+N'$, respectively to within ± 1, where N' denotes the number of real zeros of $F(s,t)$ in the interval $(0,t)$.

Case A

Case A of our crossing-symmetric model has phase contours that differ from those in Fig. 1, by having an oscillatory phase in the region $u<0$, $t<0$, giving phase contours $\pi, \pi, \pi, \cdots$, in this region also. In addition the complex zeros (dotted lines in Fig. 1) go to infinity and leave the physical sheet at values $t^1, t^2, t^3, \cdots$, which satisfy Eq. (2.2). Thus the real zeros shown in Fig. 1, become directly associated with the zeros of residues, in case A.

The reduction of F to a Herglotz function, for fixed t in case A, will give a form similar to that in Eq. (2.14), except that the order of the polynomials will now be 0, 0, and $2N$ for P_a, P_b, and P_c, respectively, to within ± 1. In case A we take the real zeros to be in one to one correspondence with the zeros of residues, so that no more than one is on the physical sheet for each negative value of t.

Further discussion of cases A and B in the complex s plane for fixed negative t is given in II. The information obtained there about the complex phase contours is necessary for the above conclusions and the reader should refer especially to II (Sec. 5) for further details.

3. PHASE CONTOURS AND FIXED-ANGLE BEHAVIOR

At a fixed angle we cannot make direct deductions from our model, either about the spacing of phase contours, or about the location of zeros, since both would require detailed assumptions about the form of the Regge trajectories, and the way in which different terms interfere. Such assumptions may be essential for a more detailed treatment but they are not appropriate to the discussion of general features with which we are concerned here. Instead we will use consistency arguments, based on the assumption that the differential cross section at fixed angle falls like some entire function for large s. Thus,

$$F(s,\cos\theta)\sim B\exp[-As^p], \qquad (3.1)$$

where the order p and the type A both depend on θ.

In case B, discussed in II (Secs. 5 and 7) and in the previous section, the real phase contours are given by Fig. 1. At fixed angle, on our assumption of dominance by Regge terms having continuously falling trajectories as t decreases, the phase $\phi(s,\cos\theta)$ increases continuously as $s\to+\infty$ along $s+i0$, for real $\cos\theta$ in $(-1,1)$. Only for $\cos\theta=\pm 1$ does the behavior change radically; then the phase tends to $\frac{1}{2}\pi$, as $s\to+\infty$. For fixed angle and negative s, along $s+i0$, the phase oscillates. Hence, from our discussion in I, and in Sec. 2 above, we would expect the rate of decrease of the amplitude, as $s\to+\infty$, to be related to the increase of the phase. There may also be zeros in $\mathrm{Im}s>0$, but for case B it is consistent to assume they are finite in number and for simplicity we assume there are none.

If the phase contours, for fixed θ, along s real and positive, ceased to cycle through multiples of 2π for $s>s_0$, for case B on the above assumptions, we would obtain

$$F(s,\cos\theta)=\frac{H(s,\cos\theta)}{P_c(s,\cos\theta)}, \qquad (3.2)$$

analogous to (2.14), where P_c is a polynomial in s of order n_0 where $n_0\pi$ denotes the phase near $s=s_0$. However, in our model the phase does not have an upper bound as $s\to+\infty$ at fixed angle of scattering, and heuristically we must therefore replace the form (3.2) by

$$F(s,\cos\theta)=\frac{H(s,\cos\theta)}{R(s,\cos\theta)}, \qquad (3.3)$$

where H is Herglotz in s, and R denotes an entire function obtained by factoring out the zeros of $\mathrm{Im}F$ on the right-hand cut in the complex s plane.

More generally, without the use of our generalized Regge model, if an amplitude $F(s,\cos\theta)$ has (i) a bounded phase as $s\to-\infty$, (ii) a finite number of zeros in $\mathrm{Im}s>0$, and (iii) an unbounded increasing phase as $s\to+\infty$, it would have the form (3.3) modified by including a polynomial in the numerator. Conversely, if (i) and (ii) hold, and we assume Eq. (3.1) on experimental grounds, we can deduce (iii).

The qualitative form of the phase contours of $F(s,\cos\theta)$ in the s plane, can be deduced from Fig. 1, with the aid of an extrapolation from the fixed-t phase contours considered in II (Sec. 5). The order of the entire function R in Eq. (3.3) can be related to the asymptotic form of the phase contours in the simple case where, for large $|s|$ near $\arg(s)=\pi$,

$$R(s,\cos\theta)\sim\exp[-A|s|^p\exp(ip\psi)], \qquad (3.4)$$

where $\psi=\arg(s)$. Then the phase contours have the asymptotic form

$$|s|^p\sin(p\psi)=\text{const}. \qquad (3.5)$$

The order of R can also be related to the density of points at which $\mathrm{Im}F=0$, with $\phi=n\pi$, for large real and positive values of s. Let $N(x)$ be the number of zeros of $\mathrm{Im}F(s,\cos\theta)$ for $0<s<x$. From its construction [discussed in I (Secs. 2 and 4)], the function R will have zeros at each of the real zeros of $\mathrm{Im}F$, and $N(x)$ will denote the number of zeros of R in $|s|<x$. Jensen's

theorem gives

$$\int_0^r \frac{N(x)dx}{x}=\frac{1}{2\pi}\int_0^{2\pi}[\ln|R(r\exp i\psi)|\,d\psi]-\ln[R(0)]. \quad (3.6)$$

R is of order p, so

$$\ln|R(r\exp i\psi)|<K(\epsilon)r^{p+\epsilon}, \quad (3.7)$$

where ϵ is any small positive number. Also,

$$\int_0^{2r}\frac{N(x)dx}{x}\geqslant N(r)\int_r^{2r}\frac{dx}{x}\geqslant N(r)\ln 2. \quad (3.8)$$

Hence

$$N(r)\leqslant\frac{1}{\ln 2}\int_0^{2r}\frac{N(x)}{x}dx<Kr^{p+\epsilon}. \quad (3.9)$$

Thus the density of phase contours

$$\phi(s,t)=n\pi, \quad (3.10)$$

in Fig. 1, is closely related to the order $p(\theta)$ of the entire function R for a fixed angle of scattering θ.

In case A, discussed in II (Secs. 5 and 7) and in Sec. 2 above, the phase $\phi(s,\cos\theta)$ has bounded oscillations along the real s axis above the branch cut. In this case the oscillations of ImF play only a minor role in the asymptotic behavior of $|F|$. If there were no zeros of $F(s,\cos\theta)$ in Im$s>0$, it would be essentially a Herglotz function, and we would have an inequality like (2.13). This is in contradiction with our model which assumes dominance by leading Regge terms in the physical region. More generally it contradicts our requirement (3.1) for a rapid decrease of cross section at fixed angle.

We conclude that in case A there must be an infinite number of zeros of $F(s,\cos\theta)$ in Im$s>0$, when $\cos\theta$ is in $(-1,1)$, but $\cos\theta\neq\pm1$. If the number of zeros was only finite, they would lead to a polynomial factor in $F(s,\cos\theta)$, like $P_a(s)$ in Eq. (2.14), which would increase the power behavior at infinity. However, an infinite number of zeros, leads to an entire function, and we obtain

$$F(s,\cos\theta)=E(s,\cos\theta)H(s,\cos\theta), \quad (3.11)$$

where E is an entire function in s.

The zeros of $F(s,\cos\theta)$ are evidently closely related to the zeros of residues in our model. They must all leave the physical sheet in the limits $\cos\theta=\pm1$. For $\cos\theta$ near to 1, say,

$$\cos\theta=1-\epsilon, \quad (3.12)$$

we can discuss the location of the zero of F that is associated with a zero of a residue, as was done for fixed real t in II (Sec. 5). The leading Regge term F_1, and the next term F_2, give

$$F(s,t)\sim F_1+F_2=F_2\left(\frac{F_1}{F_2}+1\right), \quad (3.13)$$

for large $s=s_0\exp(i\psi)$, where

$$\frac{F_1}{F_2}=\frac{\beta_1(t)}{\beta_2(t)}s_0^{(\alpha_1-\alpha_2)}\exp[i(\alpha_2-\alpha_1)(\tfrac{1}{2}\pi-\psi)]. \quad (3.14)$$

From (3.12),

$$t\approx-\tfrac{1}{2}\epsilon s_0\exp(i\psi). \quad (3.15)$$

We choose ϵ to be small, then choose s_0 large enough so that

$$-\tfrac{1}{2}\epsilon s_0=t_1^0-\epsilon', \quad (3.16)$$

where

$$\beta_1(t_1^0)=0. \quad (3.17)$$

For t near t_1^0, β_2 is negative. For $t>t_1^0$, β_1 is positive, and for $t<t_1^0$, β_1 is negative. For simplicity, we take $(\alpha_1-\alpha_2)=1$. For $\psi=0$ in Eq. (3.14), the ratio F_1 to F_2 is pure imaginary. But for $\psi>0$, from [(3.15)-(3.17)], $\beta_1(t)$ will become nearly pure imaginary even for small ψ, provided ϵ' is sufficiently small. The phase of β_1 will then cancel the phase from the exponential in Eq. (3.14). Since β_2 is negative, we obtain

$$F_1/F_2\approx-(\epsilon s_0\psi)s_0/2|\beta_2|. \quad (3.18)$$

We can choose ψ so that this ratio is a minus one, giving a zero in (3.13). As $\epsilon\to0$, this zero of $F(s,\cos\theta)$ tends to infinity in the s plane, just above the real axis.

The actual behavior of phase contours and zeros is likely to be a mixture of case B and case A. Then we would expect the high-energy behavior at fixed angles to depend on the ratio of entire functions giving

$$F(s,\cos\theta)=\frac{E(s,\cos\theta)L(s,\cos\theta)H(s,\cos\theta)}{R(s,\cos\theta)}, \quad (3.19)$$

where $L(s,\cos\theta)$ comes from real values of s where Im$F(s,\cos\theta)=0$, at which the phase ϕ is decreasing. R comes from similar values where ϕ is increasing. E comes from the zeros of F, on the physical sheet.

If the entire function E is dominant for large s, then its order must be greater than or equal to $\frac{1}{2}$. This follows from Polya's inequality, which states that

$$m(r)\geqslant[M(r)]^{\{\cos(p\pi)-\epsilon\}}, \quad \text{for large } r \quad (3.20)$$

where $m(r)$ and $M(r)$ denote the minimum and maximum values of the entire function on $|s|=r$, and p denotes its order. In defining $m(r)$, the neighborhoods of zeros are excluded. Thus, if p was less than $\frac{1}{2}$, we could deduce that $m(r)$ increases with r, and the differential cross section would increase with energy at fixed angle. We reject this on physical grounds and deduce that the order p satisfies

$$p\geqslant\tfrac{1}{2}. \quad (3.21)$$

If a smooth angular dependence is assumed we can also reject $p<\frac{1}{2}$ on the grounds that it contradicts unitarity.

4. MODULUS CONTOURS AT HIGH ENERGY

A fixed-angle lower bound was first obtained by Cerulus and Martin[3] under certain assumed uniform boundedness properties of the scattering amplitude. Their results were generalized by Chiu and Tan,[4] who discussed also their relation to rising Regge trajectories. Using analogous methods but different assumptions, Tiktopoulos and Treiman[5] have obtained certain constraints on the angular dependence of scattering amplitudes.

In this section, we discuss the characteristic features of phase contours in the z_t plane at large values of t, where t denotes the energy and z_t the cosine of the scattering angle. Using the harmonic properties of the phase and modulus contours we note how one can define a region D_∞ in the z_t plane, in which the scattering amplitude is polynomial bounded. The properties of the region D_∞ are used in Sec. 5 to provide a lower bound for fixed-angle behavior that is a generalization of earlier results.

In formulating our approach, we make use of our deductions about phase contours for the crossing-symmetric model developed in II and discussed in previous sections. Some of our conclusions are more general in character and depend only on the specific asymptotic form of certain modulus contours.

A. Phase Contours in the z_t Plane

For fixed t, the transformation from s to z_t is linear, so the topology of the phase contours will not be altered in going from the s plane to the complex z_t plane:

$$z_t=1+\frac{2s}{t-4m^2}=\frac{s-u}{t-4m^2}. \tag{4.1}$$

We consider the phase contours for real t above the branch cut $(t+i0)$, in the complex z_t plane. These are analogous to those shown in paper II, Fig. 18. Using the limit $t+i0$, the real section for $t>4m^2$ differs from that shown in Fig. 1 by (i) an interchange of the left-hand side with the right-hand side, and (ii) the $\frac{3}{2}\pi$ contours are replaced by $\frac{1}{2}\pi$ contours. The resulting complex section is shown in the z_t plane in Fig. 2, for real t corresponding to

$$3<\alpha(t)<4. \tag{4.2}$$

The asymptotic phase in the z_t plane is given by

$$\phi(t+i0, z_t)\sim\tfrac{1}{2}\pi+\alpha(t)\theta, \tag{4.3}$$

where $z_t=|z_t|\exp(i\theta)$, and $z_t\to\infty$, for $0\leqslant\theta\leqslant\pi$. This corresponds to asymptotic behavior $|z_t|^{\alpha(t)}$ of the modulus of F, for large $|z_t|$. Note that the region above the right-hand cut in the z_t plane corresponds to

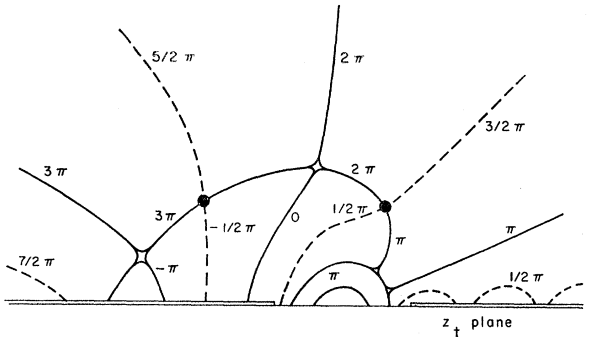

FIG. 2. Phase contours in the complex z_t plane for t real in the limit $(t+i0)$, such that $3<\alpha(t)<4$ in the crossing-symmetric model. The upper phases are obtained for a path above the zeros, the lower phases are for a path below the zeros, in both cases starting from the real axis on the right-hand side.

$\mathrm{Im}(s)>0$, whereas that above the left-hand cut corresponds to $\mathrm{Im}(u)<0$. This explains the asymmetry since t also is above threshold. In addition there is no real region where the amplitude F is also real (because $t>4m^2$), so we do not have any upper and lower half-plane symmetry.

In our model we assume that as t increases, $\alpha(t)$ increases without limit. Then, for increasing t, there will be new phase contours continuously entering the physical sheet of the z_t plane from the left-hand cut. All of these contours remain unbounded (i.e., they go to infinity) on the physical sheet.

In contrast to the phase contours from the left-hand cut, there will be a class of bounded contours coming from the region

$$-1-\frac{8m^2}{t-4m^2}<z_t<1+\frac{8m^2}{t-4m^2}. \tag{4.4}$$

These contours are associated with decreasing $\alpha(s)$ and $\alpha(u)$ in the physical t channel, as s and u became more negative.

The above unbounded and bounded types of contours are separated by the leading bounded π contour. In addition, there are $\frac{1}{2}\pi$ contours associated with the right-hand cut, but our argument does not require us to know whether these are unbounded or bounded. We denote by Δ_t the region in the z_t plane that is bounded by the leading π contour for given t.

As $t\to+\infty$, the phase contours in the real (s,t,u) plane become parallel to $u=\text{const}$, or $s=\text{const}$. Thus a particular phase contour, say

$$\phi(t,z_t)=\tfrac{1}{2}\pi+n\pi, \tag{4.5}$$

will meet the left-hand cut of the z_t plane at a point P_n given by

$$z_t=-1-\frac{2c(n)}{t-4m^2}, \tag{4.6}$$

[3] F. Cerulus and A. Martin, Phys. Letters 8, 80 (1964).
[4] C. B. Chiu and C.-I Tan, Phys. Rev. 162, 1701 (1967).
[5] G. Tiktopoulos and S. B. Treiman, Phys. Rev. 167, 1437 (1968).

where $c(n)$ is defined by

$$\alpha[c(n)]=n. \tag{4.7}$$

The phase (4.5) using (4.6) will apply out to the point in Fig. 2, where the phase contour through the sequence of zeros meets the real z_t axis. As $t\to+\infty$, this point in our model tends to $z_t=-3$ since it lies on the line $u=t$. In contrast, each point P_n, for fixed n, will approach $z_t=-1$ as $t\to+\infty$, like $(t)^{-1}$. The phase contours (4.5) will wind around the bounded π contour, and then move to infinity in their asymptotic direction in the z_t plane, found from Eq. (3.4). At the same time, for increasing t, the bounded phase contours will become denser near the limiting π contour, within the region Δ_t that it bounds.

We will assume that as $t\to+\infty$,

$$\Delta_t\to\Delta_\infty, \tag{4.8}$$

where Δ_∞ is a finite bounded region in the z_t plane. For simplicity, we assume that

$$\Delta_{t_1}\subset\Delta_{t_2}, \quad \text{if} \quad t_1<t_2. \tag{4.9}$$

Then all of the closed phase contours, for finite t, lie inside Δ_∞. The general form of the phase contours for large t is sketched in Fig. 3. As noted above, we do not expect these contours to show any symmetry with respect to $\mathrm{Im}(z_t)=0$. In particular the boundary of Δ_t will not in general meet the real axis at right angles. We denote the angles by $\theta_1(t)$ and $\theta_2(t)$ as shown in Fig. 3, and assume that they tend to values θ_1 and θ_2 in $(0,\frac{1}{2}\pi)$ as $t\to\infty$.

B. Modulus Contours in z_t Plane

The phase $\phi(s,t)$, and $\ln|F(s,t)|$, are respectively the imaginary and the real parts of $\ln[F(s,t)]$. Hence they are harmonic functions of x and y, where $z_t=x+iy$. From the properties of harmonic functions, the phase contours and the modulus contours will be mutually orthogonal in the complex z_t plane. If the phase contours are known, the modulus contours can be constructed. For example, if $|z_t|$ is large enough, the modulus contours will approximate to semicircles centered on the origin with radius $|z_t|$. The phase and modulus contours, that correspond to fixed real t such that $3<\alpha(t)<4$, are shown in Fig. 4.

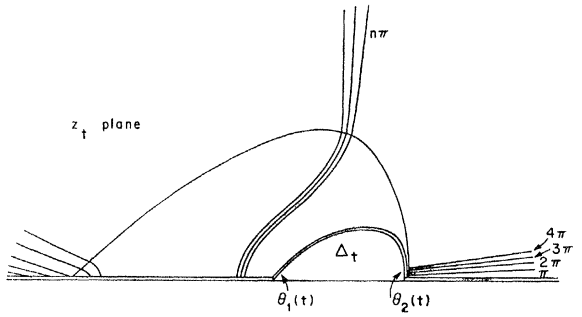

FIG. 3. Phase contours in the z_t plane in the crossing-symmetric model for large energy (t).

We will make special use of the modulus contour that goes through the thresholds at $z_t=\pm\rho$, where

$$\rho=1+8m^2/(t-4m^2). \tag{4.10}$$

This contour is given by

$$|F(t,z_t)|=|F(t,\rho)|, \tag{4.11}$$

and we will denote the corresponding curve in the z_t plane by Γ_t. Its shape will change as t is increased, and its detailed form will depend on the dynamics of the system. For our model, we expect it to approach the form Γ_∞, that is indicated in Fig. 5, enclosing an area D_∞ in the z_t plane. We expect D_∞ to enclose Δ_∞, since the modulus contours are orthogonal to the phase contours. In general the angle δ of Γ_∞ with the left-hand real axis will differ from the corresponding angle with the right-hand axis.

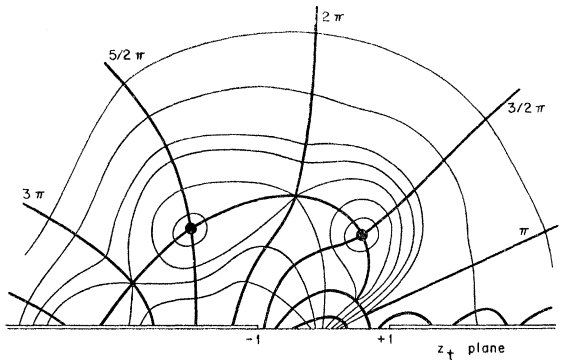

FIG. 4. Phase contours (heavy lines) and modulus contours (thin lines) for the crossing-symmetric model, in the complex z_t plane. The energy has similar value to that giving the phase contours in Fig. 2.

For $z_t{}^i$ inside D_∞ in the z_t plane, we will have

$$F(t,z_t{}^i)/t^2\to 0 \quad \text{as} \quad t\to\infty \tag{4.12}$$

since for large t,

$$|F(t,\pi)|<t^{2-\epsilon}. \tag{4.13}$$

Outside D_∞, in our model, any modulus contour $\Gamma_t(n)$, having a value t^n (with n fixed), will move towards Γ_∞ and will coincide with it in the limit $t\to\infty$. Hence at any fixed point $z_t{}^0$ outside D_∞, we will have

$$F(t,z_t{}^0)/t^n\to\infty \quad \text{as} \quad t\to\infty. \tag{4.14}$$

Thus, in our model, the modulus of the amplitude will be bounded by a polynomial in t as $t\to\infty$, for points $z_t{}^i$ inside D_∞. It will not be bounded by a polynomial for points $z_t{}^0$ outside D_∞ in the z_t plane. This suggests a need for new generalization of the results of Cerulus and Martin[3] on a fixed-angle bound. Our generalization, which we give in Sec. 5 does not depend on the special

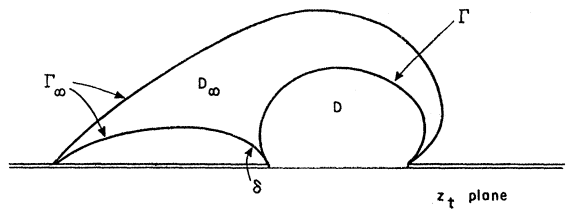

FIG. 5. The asymptotic limit Γ_∞ of modulus contours that correspond to a polynomial in the energy (t), shown in the z_t plane. The interior of Γ_∞ is the region denoted D_∞. The curve Γ is symmetric and within D_∞; it surrounds the region D.

assumptions involved in our model. However it is designed to take into account the special features and difficulties that the model indicates are likely to be associated with rising Regge trajectories, or more generally with scattering amplitudes that are not polynomial bounded.

5. FIXED-ANGLE LOWER BOUND

In the general case we assume that, for any t, there exists a region D_t of the z_t plane, within which the amplitude is polynomial bounded in the variable t. We assume that as $t\to\infty$, D_t has the limiting form shown as D in Fig. 5, and makes an angle δ with the left-hand (and right-hand) branch cuts. Let Γ_t be the boundary curve of D_t. As noted by Chiu and Tan,[4] the method of Cerulus and Martin[3] requires $\delta=0$, whereas we would in general expect δ to be nonzero.

We will make a transformation such that the image of the curve Γ_t becomes tangential to the real axis at the image of the points $z_t=\pm\rho$. Once this is done, we can then use the Cerulus-Martin theorem[6] to obtain a lower bound at fixed angle as $t\to\infty$. A transformation satisfying this requirement is given by

$$w(z_t)=\frac{[\rho^{4\alpha}-(\rho^2-z_t^2)^{2\alpha}]^{1/2}}{[\rho^{4\alpha}-(\rho^2-1)^{2\alpha}]^{1/2}}, \tag{5.1}$$

where

$$1/2\alpha=1-\delta/\pi. \tag{5.2}$$

The appropriate branch of w is the one whose inverse,

$$z_t=\{\rho^2-[\rho^{4\alpha}-(\rho^{4\alpha}-(\rho^2-1)^{2\alpha})w^2]^{\frac{1}{2}\alpha}\}^{1/2}, \tag{5.3}$$

is real analytic and Herglotz.

Consider the function

$$G(t,w)\equiv F(t,z_t). \tag{5.4}$$

It has branch points at

$$w_\rho=\pm\frac{\rho^{2\alpha}}{[\rho^{4\alpha}-(\rho^2-1)^{2\alpha}]^{1/2}}, \tag{5.5}$$

and as $t\to\infty$,

$$w_\rho\sim 1+C/t^{2\alpha}. \tag{5.6}$$

With the usual assumptions,[3,4] which include a specification of the form of D_t, we can apply the Cerulus-Martin theorem and find that

$$|F(t,z_t)|>C'\exp[-C_\alpha(z_t)t^\alpha \ln t], \tag{5.7}$$

for $-1\leqslant z_t\leqslant 1$ as $t\to\infty$. If we assume

$$0\leqslant\delta<\tfrac{1}{2}\pi(1-\epsilon), \tag{5.8}$$

we obtain

$$\tfrac{1}{2}\leqslant\alpha<1/(1+\epsilon). \tag{5.9}$$

[6] This is a generalization of the theorem proved by Cerulus and Martin which was given in Ref. 4 by Chiu and Tan. Note a minor difference between the case here and that in Ref. 4. There the function has only a right-hand cut, whereas here it has both right- and left-hand cuts. Consequently the bound here is slightly weaker, but the assumptions also are weaker.

ACKNOWLEDGMENT

We are indebted for hospitality and for helpful discussions to Professor G. F. Chew at the Lawrence Radiation Laboratory, Berkeley.